Bearings-Only Tracking and Doppler-Bearing Tracking with Inequality Constraint

Hoe Chee Lai, Rong Yang and Gee Wah Ng
DSO National laboratories
12 Science Park Drive
Singapore 118225
lhoechee@dso.org.sg,
yrong@dso.org.sg and
ngeewah@dso.org.sg

Felix Govaers, Martin Ulmke, Wolfgang Koch
Fraunhofer FKIE
Fraunhofer Str. 20, 53343
Wachtberg, Germany
felix.govaers@fkie.fraunhofer.de,
martin.ulmke@fkie.fraunhofer.de and
wolfgang.koch@fkie.fraunhofer.de

***Abstract* — This paper aims to find an appropriate approach to improve estimation accuracy of bearings-only tracking (BOT) and Doppler bearing tracking (DBT) by making use of the constraint on target speed. Targets usually travel within a valid speed zone so this contextual information (speed inequality constraint) should hypothetically help tracking algorithms (filters) achieve better accuracy. However the inequality constraint filters, usually implemented using the rejection sampling approach, have high computational cost. This paper will study the accuracy improvement brought by the inequality constraint as well as the computational cost introduced in the BOT and DBT problems. Furthermore, we will also propose cost effective approach, which is the speed and range parameterized multiple model (MM) filter with different initial states in the valid range and speed zone. This MM-BOT/DBT, inspired from the range parameterized BOT (RP-BOT), applies the speed inequality constraint at track initial stage. Simulation test results show that the MM approach outperforms others in terms of estimation accuracy and computational efficiency.**

Keywords: *Bearing-only tracking; Doppler-bearing tracking; Inequality constraint.*

1 Introduction

Passive target tracking is widely used due to its concealing property. In this paper, we focus on the passive tracking with sensors which could only measure the target bearings or in some case the target Doppler shifted frequencies. As the target range is not measurable, the target trajectory estimation is generally poor.

The most frequently used passive tracking approach is the bearings-only tracking (BOT). This approach requires the sensor platform to manoeuvre so that the target trajectory is observable (or marginal observable) [1] [2]. Although recent research shows some observable cases for non-manoeuvring sensor but the target needs to perform particular manoeuvres [3][4], it is practically difficult as target motion pattern is unknown to the sensor.

The BOT can be extended to Doppler-Bearing tracking (DBT) if the passive sensor provides the Doppler shifted frequency information [5] [6]. In general, target trajectory is observable in DBT even when the sensor platform is not maneuvering. This adds an additional element in the state to be estimated.

As the target trajectory is not accurate under marginally observable in BOT and DBT, it is worth to investigate the possible enhancement of using contextual information. In this paper, we will investigate the effects of applying the target speed inequality constraint which is given by

$$\sqrt{(\dot{x}_k^2 + \dot{y}_k^2)} \leq sp_{max} \tag{1}$$

where $\dot{x}_k$ and $\dot{y}_k$ are the target speeds in the x and y coordinates at time k, respectively; sp_{max} is the maximum speed of the target which is assumed known.

Unlike the equality constraint, the inequality constraint often suffers high computational cost when it is embedded in tracking filters, especially when the problem is marginal observable. It imposes "hard" inequality constraint on the state with large error at every time cycle in the dynamic estimation process. The large error means that more samples are needed to be generated to represent the state distribution which results in high computational cost. The commonly used algorithms include truncated unscented Kalman Filter (TUKF), unscented Kalman filter with Rejection Sampling (UKF-Rej) and Particle Filter with Rejection Sampling (PF-Rej) [8] [9] [14] [15]. They will be reviewed in Section 3.

We will also propose a cost effective algorithm, which is the speed and range parameterized multiple model (MM) filter with different initial states in the valid range and speed zone. This MM-BOT/DBT is inspired from the range parameterized BOT (RP-BOT) [10] [11]. It applies the speed inequality constraint at track initial stage. Subsequently the multiple models with different initial states running in parallel will be updated by the measurements independently. The likelihoods of the models are computed by the innovations and the final output is the weighted sum of the estimates from the individual models.

Simulation tests will be conducted on these algorithms with the inequality constraint. The most effective and cost efficient algorithm will be identified.

2 BOT and DBT problem formulation

This section gives the respective BOT and DBT problem formulation in detail.

2.1 BOT

BOT approach tracks a target using a single passive sensor that only provides bearing measurements. The problem formulation

is given next. The target state to be estimated and measurement at time k are

$$\mathrm{X}_k^{\mathrm{b}} = [x_k \quad y_k \quad \dot{x}_k \quad \dot{y}_k]' \tag{2}$$

$$\mathrm{Z}_k^{\mathrm{b}} = b_k \tag{3}$$

where x, y, $\dot{x}$ and $\dot{y}$ are the target positions and speed in the x and y coordinates, respectively. The state transition model is

$$X_k^* = \mathrm{F}_{k-1}^* \mathrm{X}_{k-1}^* + \mathrm{G}_{k-1}^* v_{k-1} \tag{4}$$

where v_{k-1} is the zero-mean white Gaussian process noise with covariance Q. The asterisk (*) stands for either b (for BOT) or d (for DBT). F^* and G^* in BOT are defined as

$$\mathrm{F}_{k-1}^{\mathrm{b}} = \begin{bmatrix} 1 & 0 & T & 0 \\ 0 & 1 & 0 & T \\ 0 & 0 & 1 & 0 \\ 0 & 0 & 0 & 1 \end{bmatrix} \tag{5}$$

$$\mathrm{G}_{k-1}^{\mathrm{b}} = \begin{bmatrix} 0.5T^2 & 0 \\ 0 & 0.5T^2 \\ T & 0 \\ 0 & T \end{bmatrix} \tag{6}$$

where T is the time interval. The measurement model is defined as

$$\mathrm{Z}_k^* = h^*(\mathrm{X}_k) + \mathrm{w}_k \tag{7}$$

where w_k is the zero-mean white Gaussian measurement noise with variance R, and

$$h^{\mathrm{b}}(\cdot) = \tan^{-1}\left(\frac{\Delta x_k}{\Delta y_k}\right) \tag{8}$$

with Δx_k and Δy_k are the relative distances between the sensor and target in the x and y coordinates respectively.

2.2 DBT

In certain cases, the passive sensor will also be able to measure the Doppler frequency of the target in addition to the bearing measurement. This additional measurement is able to provide extra radial velocity information to the tracker. The target state and measurement for the DBT are

$$\mathrm{X}_k^{\mathrm{d}} = [x_k \quad y_k \quad \dot{x}_k \quad \dot{y}_k \quad f_k^{\mathrm{e}}]' \tag{9}$$

$$\mathrm{Z}_k^{\mathrm{d}} = [b_k \quad f_k^{\mathrm{d}}]' \tag{10}$$

where f^{e} is the unknown target emitting frequency (assumed constant) and f_k^{d} is the Doppler shifted frequency.

The state transition model and measurement model have been given in (4) and (7) respectively. However due to the additional Doppler frequency information, the $\mathrm{F}^*, \mathrm{G}^*, \mathrm{R}^*$ and $h^*(\cdot)$ are slightly different and are defined as

$$\mathrm{F}_{k-1}^{\mathrm{d}} = \begin{bmatrix} 1 & 0 & T & 0 & 0 \\ 0 & 1 & 0 & T & 0 \\ 0 & 0 & 1 & 0 & 0 \\ 0 & 0 & 0 & 1 & 0 \\ 0 & 0 & 0 & 0 & 1 \end{bmatrix} \tag{11}$$

$$\mathrm{G}_{k-1}^{\mathrm{d}} = \begin{bmatrix} 0.5T^2 & 0 & 0 \\ 0 & 0.5T^2 & 0 \\ T & 0 & 0 \\ 0 & T & 0 \\ 0 & 0 & 1 \end{bmatrix} \tag{12}$$

$$h^{\mathrm{d}}(\cdot) = \begin{bmatrix} \tan^{-1}\left(\frac{\Delta x_k}{\Delta y_k}\right) \\ f_k^{\mathrm{e}}\left(1 - \frac{\dot{r}_k}{c^{\mathrm{p}}}\right) \end{bmatrix} \tag{13}$$

where c^{p} is the speed of propagation of the signal, and $\dot{r}_k$ is the radical velocity between the target and the sensor at time k. The radical velocity is given by:

$$\dot{r}_k = \frac{\Delta x_k \Delta \dot{x}_k + \Delta y_k \Delta \dot{y}_k}{\sqrt{\Delta x_k^2 + \Delta y_k^2}} \tag{14}$$

where $\Delta \dot{x}_k$ and $\Delta \dot{y}_k$ are the relative speeds between the sensor and target in the x and y coordinates.

3 Tracking Algorithms with constraint

This section describes five tracking algorithms with inequality constraint that will be tested in this paper. The first three algorithms (TUKF, UKF-Rej and PF-Rej) use "hard" constraint on the state in each time cycle. The fourth algorithm, RP-BOT/DBT, uses multiple initial states with different target ranges in the valid zone. It can be viewed as applying the inequality constraint about the target range at initial stage. The fifth algorithm is the MM-BOT/DBT proposed in this paper. It extends RP-BOT/DBT to include speed-parameterized initialization in multiple models, so that the speed inequality constraint is utilized in the initial stage.

3.1 Truncated Unscented Kalman Filter

The truncated unscented Kalman filter (TUKF) [8] consists of three steps, namely the prediction, update and truncation. The prediction and update are the same as the normal UKF [12] which estimates the posterior state and its error covariance $\breve{\mathrm{X}}_k$ and $\breve{\mathrm{P}}_k$ at time k. The truncation step is done by adjusting the posterior sigma points to satisfy the inequality constraint. The final state mean and error covariance $\hat{\mathrm{X}}_k$ and $\hat{\mathrm{P}}_k$ are then computed by the adjusted sigma points. This procedure is also called PDF truncation [13].

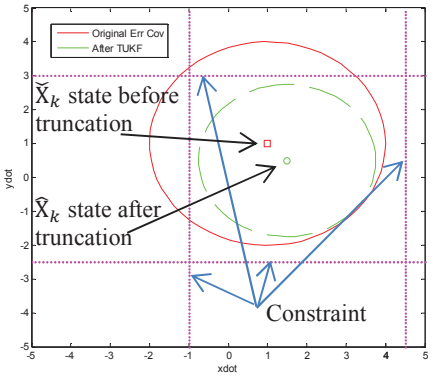

Figure 1. State mean and error covariance before and after PDF truncation

Figure 1 shows the state mean and error covariance before (red line) and after truncation (green dotted line). The constraints used in this example are $-1\text{m/s} \le \dot{x} \le 4.5\text{m/s}$ and $-2.5\text{m/s} \le \dot{y} \le 3\text{m/s}$.

3.2 UKF with Rejection Sampling

UKF with Rejection sampling [9] is similar to TUKF whereby it is also a three step algorithm with the prediction, update and truncation. The prediction and update are the same as the normal UKF [12] while the truncation step is described below.

A predetermined number of samples will be randomly drawn from the posterior state estimated by the normal UKF (with mean and error covariance $\breve{\mathrm{X}}_k$ and $\breve{\mathrm{P}}_k$, respectively). Each of the samples is then compared against the constraint and only those samples satisfied the constraint is accepted. The final $\hat{\mathrm{X}}_k$ and $\hat{\mathrm{P}}_k$ are then computed from the accepted samples. However, this approach only works well when the sample size is sufficiently large and acceptance rate is high.

Figure 2 shows the samples before (in blue) and after applying rejection sampling (in red). The constraint used in this example is the maximum target speed must be less than 30m/s.

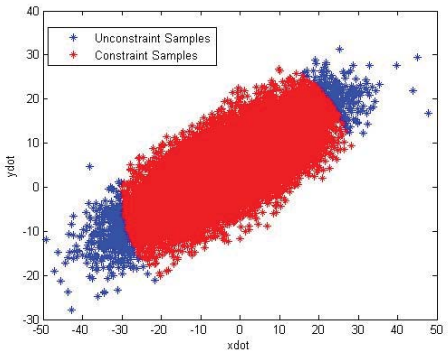

Figure 2. Samples before and after Rejection Sampling

3.3 Particle Filter with Rejection Sampling

Particle Filter (PF) uses a large number of weighted particles to represent the state PDF. It is a Monte Carlo (sampling) method and can cope with nonlinear and non-Gaussian problem but it involves high computational cost. The number of particles has no upper bound but typically increases exponentially with the dimension of target state. However with more particles generated, the computational cost will be compromised [14] [15].

Rejection sampling described in the subsection 3.2 can be easily incorporated into PF by checking if each particle satisfies the constraint at every time cycle. This constraint checking should be inserted in the calculation of the particle weights. If a particle does not satisfy the constraint, its corresponding weight will be set to zero. This is done before the normalization of the particle weights.

3.4 Range Parameterized BOT/DBT

The basic idea of Range-parameterized BOT/DBT (RP-BOT/DBT) [10] [11] is to use multiple models to handle the large uncertainty of target range at the initial stage. Each of the models has different initial state estimated from possible ranges. These ranges can be uniformly distributed within the interval of range interest (r_{min}, r_{max}).

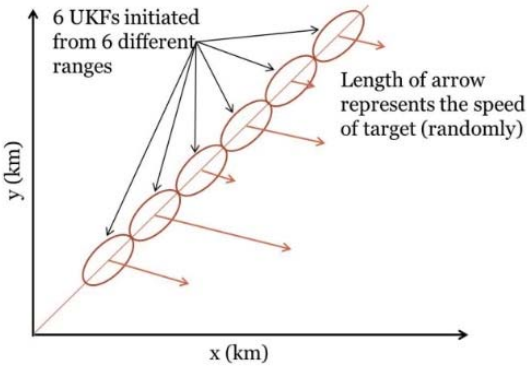

Figure 3. Range subinterval initialization diagram

Figure 3 shows the range subinterval initialization diagram in Cartesian coordinates based on the first bearing measurement. Six UKFs are initiated from six ranges uniformly distributed in detection range.

The initial state of model *m* for the BOT is:

$$\mathrm{X}_1^{\mathrm{b}(m)} = \begin{bmatrix} x_1^s + r^{(m)}\sin(b_1) \\ y_1^s + r^{(m)}\cos(b_1) \\ s\sin(c) \\ s\cos(c) \end{bmatrix} \tag{15}$$

where b_1 is the first measured bearing, s is the initial speed drawn from a Gaussian PDF $s \sim N(\bar{s}, \sigma_s^2)$, c is the initial course drawn from a Gaussian PDF $c \sim N(\bar{c}, \sigma_c^2)$ where $\bar{s}, \bar{c}, \sigma_s^2, \sigma_c^2$ are the means and variances of the target speed and course, respectively. The initial state error covariance is

$$\mathrm{P}_1^{\mathrm{b}(m)} = \begin{bmatrix} P_{xx} & P_{xy} & 0 & 0 \\ P_{yx} & P_{yy} & 0 & 0 \\ 0 & 0 & P_{\dot{x}\dot{x}} & P_{\dot{x}\dot{y}} \\ 0 & 0 & P_{\dot{y}\dot{x}} & P_{\dot{y}\dot{y}} \end{bmatrix} \tag{16}$$

where

$$P_{xx} = (r^{(m)}\sigma_b cos(b_1))^2 + (\sigma_r \sin(b_1))^2 \tag{17}$$

$$P_{yy} = \left(r^{(m)}\sigma_b \sin(b_1)\right)^2 + (\sigma_r \cos(b_1))^2 \tag{18}$$

$$P_{xy} = P_{yx} = \left(\sigma_r^2 - \left(r^{(m)}\sigma_b\right)^2\right)\sin(b_1)\cos(b_1) \tag{19}$$

$$P_{\dot{x}\dot{x}} = (s\sigma_c \cos(c))^2 + (\sigma_s \sin(c))^2 \tag{20}$$

$$P_{\dot{x}\dot{x}} = (s\sigma_c \cos(c))^2 + (\sigma_s \sin(c))^2 \tag{21}$$

$$P_{\dot{x}\dot{y}} = P_{\dot{y}\dot{x}} = (\sigma_s^2 - (s\sigma_c)^2)\sin(c)\cos(c) \tag{22}$$

As for the DBT, the equations for calculating the initial target state and error covariance are similar to BOT except there is an

additional emitting frequency parameter (f^{e}) augmented in the state to be estimated. The initial state and its error covariance are

$$\mathrm{X}_1^{\mathrm{d}(m)} = \begin{bmatrix} x_1^{\mathrm{s}} + r^{(m)} \sin(b_1) \\ y_1^{\mathrm{s}} + r^{(m)} \cos(b_1) \\ s \sin(c) \\ s \cos(c) \\ f^{\mathrm{e}} \end{bmatrix} \tag{23}$$

$$\mathrm{P}_1^{\mathrm{d}} = \begin{bmatrix} P_{xx} & P_{xy} & 0 & 0 & 0 \\ P_{yx} & P_{yy} & 0 & 0 & 0 \\ 0 & 0 & P_{\dot{x}\dot{x}} & P_{\dot{x}\dot{y}} & 0 \\ 0 & 0 & P_{\dot{y}\dot{x}} & P_{\dot{y}\dot{y}} & 0 \\ 0 & 0 & 0 & 0 & P_f \end{bmatrix} \tag{24}$$

where P_f is the error covariance of the emitting frequency and f^{e} is the initial frequency measurement.

The subsequent recursive estimation will follow the static multiple model (MM) estimator [16].

The RP-BOT/DBT can be viewed as putting the inequality constraint of target range (within $[r_{min}, r_{max}]$) in its initial stage. The static MM can "softly" adapt the final state to the correct model (or the models with initial state close to the ground truth) in a Bayesian sense.

3.5 Multiple Model BOT/DBT

We extend the RP-BOT/DBT to range and speed parameterized approach so that the inequality constraint of target speed is utilized in the initial stage. We name it Multiple Model BOT/DBT (MM-BOT/DBT) in this paper.

It runs a number of independent models in parallel, and each model is initialized with a different range and speed estimates. Similarly, speed interval of interest (sp_{min}, sp_{max}) will be divided into the predefined number of subintervals.

Figure 4 shows the range and speed parameterized initialization diagram. There are twelve UKFs initiated from six ranges and two speeds (fast and slow) in this example. The number of models is doubled compared to the range parameterized algorithm.

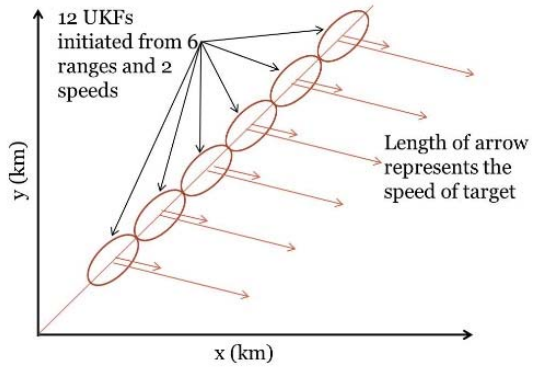

Figure 4. Range and speed subinterval initialization diagram

In order to reduce the computational cost introduced by more models, model reduction mechanism is implemented. This is because in majority of scenarios, the mode probability of mismatched models will reduce to near zero over time. These mismatched models can be removed from the model set without much loss in accuracy. The model will be removed if it satisfies the following condition

$$(w_k^{(m)} \leq thd_w) \cap (k \geq thd_t) \tag{25}$$

where $w_k^{(m)}$ is the mode probability of model m at time k, thd_w and thd_t are the predefined thresholds for mode probability and time respectively.

4 Simulation

This section demonstrates the performance of the passive tracking algorithms with inequality constraint mentioned in Section 3 through simulation. It is separated into four subsections, namely, test scenario, track initiation and parameter setting, RMSE and computation time.

4.1 Test Scenario

The test scenario is presented in Figure 5. It simulates a surface target moving at a constant speed of 7m/s and a platform (where the sensor is mounted) moving at a constant speed of 5m/s. The platform makes a 90° right turn at the middle of the whole path. The turn rate is 9°/s. The total duration is 130s. The passive sensor sampling interval is 1s. The emitting frequency f^{e} is set as a constant 100Hz. The measurement errors of bearing and Doppler frequency are assumed zero-mean white Gaussian with standard deviations $\sigma^b = 1°$ and $\sigma^f = 0.01$Hz respectively.

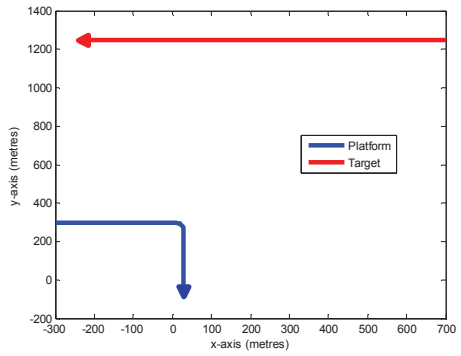

Figure 5. Test scenario to simulate a platform and target

4.2 Track Initiation and Parameter Setting

Table I shows the algorithms applied on the BOT or DBT problem in the testing. The maximum speed is set to 30m/s in the inequality constraint (1). 100 Monte Carlos runs are conducted for getting the results.

TABLE I. SUMMARY OF ALGORITHMS AND THEIR DESCRIPTIONS

Algorithm	Description
BOT/DBT	UKF without constraints.
BOT/DBT-TUKF	Truncated UKF to handle inequality constraint.
BOT/DBT-Rej	UKF with rejection sampling using 25k samples
PF-Rej (1k)	PF with rejection sampling using 1k particles.
PF-Rej (20k)	PF with rejection sampling using 20k particles.
RP-BOT/DBT	Range-parameterized approach (with 6 models)
MM-BOT/DBT	Range and speed parameterized approach (with dynamic models ≤ 12).

The following describes the track initialization and parameters setting for each algorithm.

- **BOT/DBT,BOT/DBT-TUKF,BOT/DBT-Rej**
  The initial state and its error covariance are computed by (15)-(16) for BOT and (23)-(24) for DBT, where range r, speed s, and course c are randomly selected from [0m 18km], [0m/s 30m/s] and [0° 360°] in each run respectively.
- **PF-Rej(1k),PF-Rej(20k)**
  The initial particles are computed by r, s, c which are randomly selected from [0m 18km], [0m/s 30m/s] and [0° 360°] in each run respectively.
- **RP-BOT/DBT**
  The algorithm is initialized with six models and each model with different initial ranges from
  $r \in [3\text{km} \quad 6\text{Km} \quad 9\text{Km} \quad 12\text{Km} \quad 15\text{Km} \quad 18\text{Km}]$
  s is randomly drawn from [0m/s 30m/s]
  $$c = \begin{cases} b_1 + \dfrac{\pi}{2} & (b_{10} \geq b_1) \\ b_1 - \dfrac{\pi}{2} & (b_{10} < b_1) \end{cases}$$
- **MM-BOT/DBT**
  The algorithm is initialized with twelve models, each computed by the following initial range, speed and course
  $r \in [3\text{Km} \quad 6\text{Km} \quad 9\text{Km} \quad 12\text{Km} \quad 15\text{Km} \quad 18\text{Km}]$
  $s \in [7m/s \quad 25m/s]$
  $$c = \begin{cases} b_1 + \dfrac{\pi}{2} & b_{10} \geq b_1 \\ b_1 - \dfrac{\pi}{2} & b_{10} < b_1 \end{cases}$$
  The thresholds for model reduction are set as $\text{thd}_\text{w} = 0.01$ and $\text{thd}_\text{t} = 80\text{s}$.

4.3 RMSE

The position estimate RMSEs of all the algorithms and CRLB standard deviations (s.d.) versus time for the BOT and DBT are shown in Figure 6 and Figure 7, respectively. The starting time is 70s when the platform completes its 90° turn, so that the problem is observable. The accuracy improvement of the algorithms with inequality constraint over the BOT/DBT is summarized in Table II.

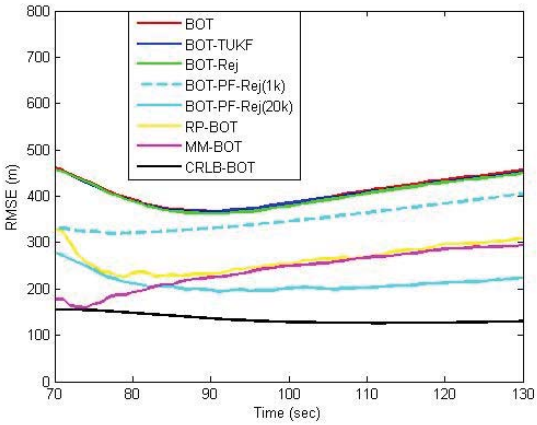

Figure 6. Position estimate RMSE and CRLB s.d. versus time for the BOT

From Figure 6 and Figure 7, it can be seen that the RMSE improvement of the BOT/DBT-TUKF and BOT/DBT-Rej over BOT/DBT is not significant, although both of them use the speed information in the constraint (less than 30m/s). This is because the inequality constraint is incorporated during the initialisation while the subsequent estimates is based on a small process noise and measurements do not bring the states out of the constraint much. The inequality "hard" constraint is not very effective.

As for the RP-BOT/DBT and MM-BOT/DBT, the improvement is superior to the TUKF and Rej approaches. These multiple model approaches only apply the constraint in the track initiation, not in the subsequent updates. From the results of the TUKF and Rej, we have observed that the inequality constraint in the update has limited effect therefore it is unnecessary to apply the "hard" constraint in the updates. The good performance of the RP-BOT/DBT and MM-BOT/DBT is brought from fast convergence to the correct models. We also observed that MM-BOT/DBT (initiated from parameterized range and speed) outperforms RP-BOT/DBT (initiated from parameterized range only) as more models are deployed.

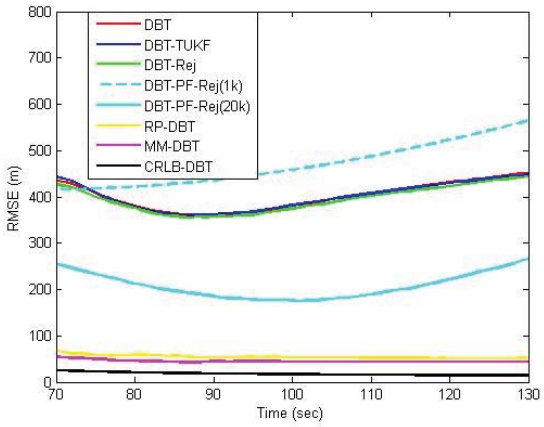

Figure 7: Position estimate RMSE and CRLB s.d. versus time for the DBT

Table II. SUMMARY OF POSITION ESTIMATE RMSE PERCENTAGE IMPROVEMENT AGAINST THE ORIGINAL BOT/DBT

BOT Algo. with constraint	RMSE impv. over BOT	DBT Algo. with constraint	RMSE Impv. over DBT
BOT-TUKF	0.65%	DBT-TUKF	0.15%
BOT-Rej	1.33%	DBT-Rej	1.68%
BOT-PF-Rej(1k)	13.22%	DBT-PF-Rej(1k)	-4.12%
BOT-PF-Rej(20k)	48.36%	DBT-PF-Rej(20k)	49.99%
RP-BOT	35.4%	RP-DBT	86.51%
MM-BOT	40.25%	MM-DBT	88.79%

The accuracy of the PF highly depends on the number of particles. Obviously, it is not enough of using 1k particles for the BOT/DBT problems. The PF with 20k particles provides the best accuracy (48.36% improvement in Table II) in BOT problem. However, with state size increases from four to five for DBT problem, its accuracy is much worse than the RP-DBT and MM-DBT. To achieve similar performance, the number of particles should increase exponentially.

4.4 Computation Time

Table III lists the computation time required by each algorithm, which are computed based on MATLAB implementation on a dual-core computer. The time stated in the table is the computer running time throughout the whole scenario (130 time cycles). Only the algorithms of BOT are shown in Table III as DBT result is similar.

Table III. COMPUTATION TIME FOR EACH ALGORITHM

Algo.	Time (s)
BOT	0.0365
BOT-TUKF	0.0388
BOT-Rej	5.7123
BOT-PF-Rej(1k)	2.8012
BOT-PF-Rej(20k)	68.787
RP-BOT	0.2069
MM-BOT	0.2665

As seen from the table above, BOT-PF-Rej(20k) is the most expensive algorithm, followed by BOT-Rej and BOT-PF-Rej(1k). They are not suitable for time critical systems. The RP-BOT and MM-BOT are 5-7 times slower than the BOT but they are much faster than the PF and rejection sampling approach (28-332 times faster). Considering the large accuracy improvement brought by RP-BOT and MM-BOT, it is a worthwhile price. Furthermore, the MM-DBT does not increase the computational cost much over the RP-BOT due to the model reduction mechanism.

5 Conclusion

This paper conducted a study on the existing dynamic estimation algorithms with inequality constraint for the BOT and DBT problems. It also proposed a cost effective speed and range parameterized multiple model (MM) filter with different initial states in the valid range and speed zone. Simulation tests were conducted to demonstrate the performance of these filters. From the results, we realized that the "hard" inequality constraint on target speed applied on the recursive update does not improve the estimation accuracy much, when the initial state is already in the valid zone. The PF performance highly depends on the number of particles, and involves high computational cost with more particles, e.g. 20k. After considering the estimation accuracy and computational time, the MM approach outperforms the others.

References

[1] Aidala, V. J., "Kalman filter behavior in bearing-only tracking applications" IEEE Tractions on Aerospace and Electronic Systems, 15, 1 (Jan. 1979, 29-39).

[2] Lindgren, A. G and Gong, K. F., "Position and velocity estimation via bearing observations" IEEE Transactions on Aerospace and Electronic Systems, 14, 4 (Jul. 1978) 564-577

[3] Clavard, J., Pillon, D., Pignol, A-C. and Jauffret, C., "Target motion analysis of a source in a constant turn from a nonmaneuvering observer" IEEE Transactions on Aerospace and Electronic Systems, 49, 3 (Jul. 2013), 1760-1780

[4] Jauffret, C. and Pillon, D., "Observability in passive target motion analysis" IEEE Transactions on Aerospace and Electonic Systems, 3, 4 (Oct. 1996), 1290-1300

[5] Jauffret, C. and Bar-Shalom, Y., "Track Formation with Bearing and Frequency Measurements in Clutter" IEEE Transactions on Aerospace Electronic Systems, 26, 6 (Nov. 1990), 999-1009

[6] Passerieux, J. M., Pillon, D., Blanc-Benon, P. and Jauffret. C., "Target Motion Analysis with Bearing and Frequencies Measurements" Proceedings of the 22nd Asilomar Conference, Pacific Grove, CA, USE, Nov. 1998

[7] Ristic B., Arulampalam S., Gordon N., "Beyond the Kalman Filter: Particle Filters For Tracking Applications" Artech House Publishers, 2004

[8] Teixeira B. O. S., Torres L. A. B., Aguirre L. A. and Bernstein D. S. "Unscented Filtering for Interval-Constrained Nonlinear Systems" 47th IEEE Conference on Decision and Control, Dec. 2008, 5116-5121

[9] G. Battistello, M. Mertens, M. Ulmke, W. Koch. Context exploitation for target tracking. In L. Snidaro, J. Garcia, J. Llinas, and E. Blasch, (editors), Context enhanced Information Fusion, pages 297–338. Springer, 2016.

[10] Peach N., "Bearing-only tracking using a set of range-parameterised extended Kalman filters" IEEE Proceedings Control Theory and Applications, 1995, Vol. 142, no. 1, 73-80

[11] Scala L. B. and Morelande M., "An Analysis of the Single Sensor Bearing-Only Tracking Problem" 11th International Conference on Information Fusion, Jul. 2008

[12] Julier S. J. and Uhlmann J. K., "A New Extension of the Kalman Filter to Nonlinear Systems", In Proceedings of AeroSense: The 11th Int. Symp. On Aerospace/Defence Sensing, Simulation and Controls, 1997

[13] Simon, D., "Optimal State Estimation: Kalman, H_∞ and Nonlinear Approaches. Wiley-Interscience, 2006

[14] Arulampalam M. S., Maskell S., Gordon N. and Clapp T., "A tutorial on particle filters for online nonlinear/non-gaussian Bayesian tracking" IEEE Transactions on Signal Processing 50(2), 2002, 174-188

[15] Carpenter J., Clifford P., Fearnhead P., "Improved particle filter for non-linear problems" IEE Proceedings Part F: Radar and Sonar Navigation, vol 146, 1999, 2-7

[16] Bar-Shalom, Y., Willett P. k., Tian, X., "Tracking and Data Fusion: A Handbook of Algorithms, YBS Publishing, 2011